Power Electronic Systems
Laboratory

Proceedings of the 35th IEEE Applied Power Electronics Conference and Exposition (APEC 2020)

Transient Calorimetric Measurement of Ferrite Core Losses

P. Papamanolis,
T. Guillod,
F. Krismer,
J. W. Kolar

Eidgenössische Technische Hochschule Zürich
Swiss Federal Institute of Technology Zurich

Transient Calorimetric Measurement of Ferrite Core Losses

Panteleimon Papamanolis, Thomas Guillod, Florian Krismer, and Johann W. Kolar

Power Electronic Systems Laboratory (PES)
ETH Zurich, Physikstrasse 3
8092 Zurich, Switzerland
Email: papamanolis@lem.ee.ethz.ch

***Abstract*—An accurate and fast transient calorimetric ferrite core-loss measurement method is proposed in this paper. In contrast to electrical measurements, the accuracy of the calorimetric approach is independent of the magnetic excitation and operating frequency. However, an accurate value of the thermal capacitance of the Core Under Test (CUT) is required, which can be achieved, e.g., by measuring the specific heat capacity of the measured core material using a Differential Scanning Calorimeter (DSC) or by using the CUT as a DC electric conductor and measuring its thermal response for known Joule heating. The proposed method is tested experimentally and compared successfully to a state-of-the-art electrical loss measurement method on MnZn ferrite cores.**

I. Introduction

Latest GaN power semiconductors are enabling very high switching frequencies and efficiencies of power electronics converters. Accordingly, the accurate computation of the losses of magnetic components of the converter circuits up to the MHz range is of great interest. This is particularly challenging for the core losses, whose behavior is highly non-linear, e.g., with respect to frequency, temperature, AC flux density and DC premagnetization. Such non-linear dependencies apply especially to ferrite materials, MnZn (20-2000 kHz) and/or NiZn (1-50 MHz), which are best suited for high frequency operation.

The main existing core loss measurement methods can be classified into electrical and calorimetric approaches [1]. Common problems to electrical methods, e.g., poor power factor and limitation to sinusoidal excitation have been resolved in [2]–[8]. State-of-the-art electrical methods feature partial cancellation of the phase-discrepancy error using an air-core inductor or a high-Q capacitor, in order to ensure adequate accuracy also at high frequencies, i.e., in the MHz range [9], [10]. However, the requirement of precise pre-calibration, elaborate post-processing and difficulties arising from dealing with parasitics remain as drawbacks.

A steady-state calorimetric measurement [11]–[13] presents a competitive alternative approach, however, the time needed for every single measurement is very long, i.e., typically in the range of several tens of minutes. In a first attempt to reduce the measurement time, a transient calorimetric measurement procedure for the core losses of magnetic components is proposed in [14]. However, the presented approach requires a complex setup with an additional "calorimeter block", which refers to a block of known mass and thermal heat capacity (e.g., copper). The magnetic component is thermally well connected to the block and the total losses (both coil and core losses) can be measured through the rate of rise of the temperature of the copper block. In addition to its complexity, the proposed method requires calibration measurements in order to identify the heat flux leaking through the insulation. A simpler method to identify the core losses in a transient calorimetric approach is introduced in [15], which mainly relies on the correlation between the core losses and the rate of change of the core temperature. However, the method has not been used to determine the absolute values of the core losses, i.e., only the relative increase of the core losses in presence of different levels of DC premagnetization has been acquired.

In this paper, the method presented in [15] is further improved, and by accurate knowledge of the thermal capacitance of the core, acquisition of the absolute value of the core losses is achieved within a short measurement time of several seconds. The operating principle of the proposed measurement method is detailed in **Section II**. The implications of measurement inaccuracies on the measured core losses are analyzed in **Section III** and the results of this analysis are verified by means of FEM simulations in **Section IV**. Finally, in **Section V**, experimental results are presented for the investigated transient calorimetric method and a state-of-the-art electric method. A comparison reveals good matching of the results obtained with the two different methods at all considered operating points, with average and maximum absolute deviations of 5.0 % and 13.0 %, respectively.

II. Experimental Setup and Operating Principle

Fig. 1 depicts the setup that consists of the Core Under Test (CUT), an enclosure that ensures steady ambient conditions (e.g., homogeneous temperature, absence of air-flow), and a reference temperature

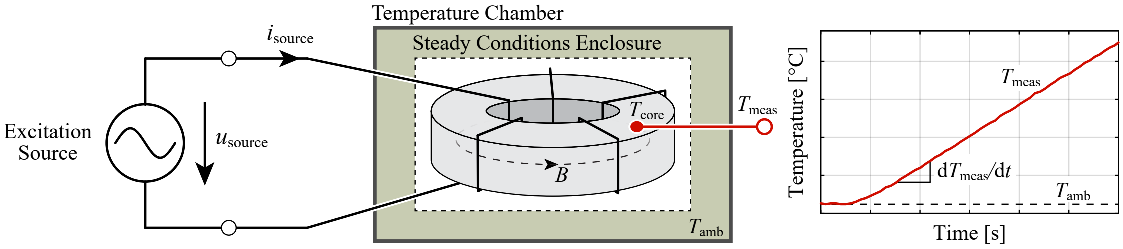

Fig. 1. (a) Proposed transient calorimetric core loss measurement setup: Core Under Test (CUT) with temperature sensor, enclosure (to achieve steady ambient conditions), and temperature chamber. (b) Example of the acquired increase of the core temperature over time.

chamber, preferably an oven, that can elevate the ambient temperature, T_{amb}, to the desired value. Finally, a high accuracy temperature sensor is attached to the core (cf. Fig. 1).

A. Fundamental measurement principle

For a given excitation and a negligible heat flux to the ambient, the temperature of the core increases according to

$$P_{\text{core}} = C_{\text{th,core}} \frac{\mathrm{d}T_{\text{core}}}{\mathrm{d}t} \approx C_{\text{th,core}} \frac{\Delta T_{\text{meas}}}{\Delta t}, \tag{1}$$

where $C_{\text{th,core}}$ is the thermal capacitance of the core, T_{core} is the core temperature, and T_{meas} denominates the temperature reading.

According to (1), the correlation between the measured losses and the temperature only depends on the thermal capacitance of the core and not on the shape of the core or on the particular waveform of the flux density in the core. Compared to high-accuracy electric measurement procedures, time consuming steps that need to be conducted for each operating point, e.g., calibration of the setup and adaptation of the components for compensation, depending on the operating point [5]–[10], are avoided.

B. Equivalent thermal network

Fig. 2(a) depicts the considered equivalent thermal network of the experimental setup. The CUT is represented by the source of losses, P_{core}, and its thermal elements, $R_{\text{th,core}}$ and $C_{\text{th,core}}$. The thermal resistance $R_{\text{th,leak}}$ models the heat leaking from the core to the ambient and to the coil through the mechanisms of thermal conduction, convection, and radiation. The setup employs two temperature sensors, i.e., the NTC thermistor,[1] considered with $R_{\text{th,NTC}}$ and $C_{\text{th,NTC}}$ in Fig. 2(a), and an IR camera. However, the IR camera actually is not required for the measurement of the core losses; it is used only for the purpose of verification of the equivalent thermal network and the employed models.

[1]From an evaluation of different temperature sensors, also including RTD and thermocouple sensors, the NTC thermistor has been selected due to its high immunity against induced electrical noise and the comparably fast response.

This network can be simplified based on the following, experimentally supported (cf. Sec. III), considerations.

- $R_{\text{th,core}}$ core is assumed to be negligible (≈ 0), due to the relatively high thermal conductivities of MnZn and NiZn ferrite core materials ($\lambda \geq 3.5\,\text{W/mK}$, cf. Sec. III-E).
- The NTC thermistor is represented by a low-pass filter with a time constant of τ_{NTC}, since $C_{\text{th,NTC}} \ll C_{\text{th,core}}$ applies.
- $C_{\text{th,core}}$ is assumed to be constant during the course of a single experiment (cf. Sec III-D).

Fig. 2(b) shows the resulting simplified equivalent circuit, which is used for the thermal analysis.

During the heating phase ($t \in [t_{\text{on}}, t_{\text{off}}]$ in **Fig. 3**), temperature independent core losses are assumed and the core temperature increases,

$$T_{\text{core}}(t) = T_{\text{amb}} + P_{\text{core}} R_{\text{th,leak}} \left(1 - \mathrm{e}^{-\frac{t - t_{\text{on}}}{R_{\text{th,leak}} C_{\text{th,core}}}}\right). \tag{2}$$

During the cooling phase ($t > t_{\text{off}}$ in Fig. 3), zero core losses apply and the core temperature converges to the ambient temperature,

$$T_{\text{core}}(t) = T_{\text{amb}} + (T_{\text{max}} - T_{\text{amb}})\, \mathrm{e}^{-\frac{t - t_{\text{off}}}{R_{\text{th,leak}} C_{\text{th,core}}}}. \tag{3}$$

According to (6), the values of $R_{\text{th,leak}}$ and $C_{\text{th,core}}$ are required for the computation of the core losses. $C_{\text{th,core}}$ depends on the mass of the core and its specific heat capacity, which is a material property that can be acquired in advance using the methods discussed in Sec. III-A. $R_{\text{th,leak}}$ depends on various factors, including the CUT, the coil, and the ambient conditions, and is estimated after each modification of the experimental setup.

For the estimation of $R_{\text{th,leak}}$, two dedicated temperature values of the cooling phase ($t_{\text{off}} < t_2 < t_2 + \Delta t_2$) of the acquired temperature profile, i.e., $T_{\text{meas}}(t_2)$ and $T_{\text{meas}}(t_2 + \Delta t_2)$ are required. The resulting equation for $R_{\text{th,leak}}$ is

$$R_{\text{th,leak,est}}(t_2, \Delta t_2) = -\frac{\Delta t_2}{C_{\text{th,core}}} \left[\ln\left(\frac{T_{\text{meas}}(t_2 + \Delta t_2) - T_{\text{amb}}}{T_{\text{meas}}(t_2) - T_{\text{amb}}}\right)\right]^{-1}. \tag{4}$$

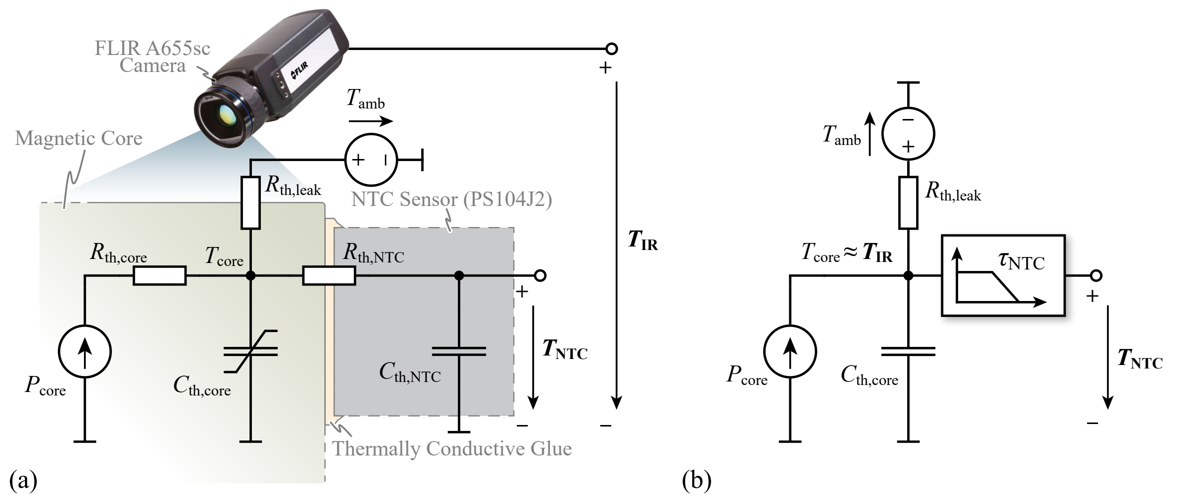

Fig. 2. (a) Equivalent circuit of the calorimetric experimental setup, including the Core Under Test (CUT), the attached NTC thermistor, and the high accuracy IR camera; (b) simplified version of the proposed equivalent circuit that is used for the rest of the analysis. The IR camera serves only for model verification and is not required for the measurement of the core losses.

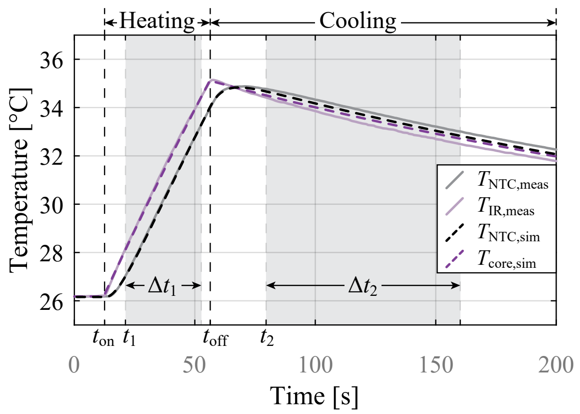

Fig. 3. Comparison of the results of a real measurement and a simulation of the equivalent network of Fig. 2(b) using a toroidal ferrite core (R 22.1/13.7/7.9, N49) that is subject to a sinusoidal magnetic flux (100 mT, 500 kHz). The core temperature is measured with a NTC thermistor (Littelfuse PS104J2 [16]) and an IR camera (FLIR A655sc [17]) at 30 frames/sec. The component values of the simulated circuit are: $P_{core} = 1.54\,\mathrm{W}$, $C_{th,core} = 7.3\,\mathrm{J/K}$, $R_{th,leak} = 45\,\mathrm{K/W}$, $\tau_{NTC} = 5.5\,\mathrm{s}$.

Finally, P_{core} is estimated using two dedicated temperature values of the waveform acquired during the heating phase, $T_{meas}(t_1)$ and $T_{meas}(t_1 + \Delta t_1)$, with $t_{on} < t_1 < t_1 + \Delta t_1 < t_{off}$,[2]

$$P_{core}(t_1, \Delta t_1) = \frac{T_{meas}(t_1 + \Delta t_1) - T_{meas}(t_1)}{\left(e^{-\frac{t_1}{R_{th,leak} C_{th,core}}} - e^{-\frac{t_1 + \Delta t_1}{R_{th,leak} C_{th,core}}} \right) R_{th,leak}}. \quad (5)$$

[2]In an alternative approach, the measured waveform could be processed by means of a Least Mean Square (LMS) approximation, in order to identify $R_{th,leak}$ and P_{core} by fitting (3) and (6) respectively. However, this would be computationally more demanding. The difference between LMS approximation and the described two-points approach is found to be consistently below 1 %.

C. Validation of the thermal network

The proposed equivalent model has been verified for a toroidal core with N49 MnZn ferrite material (EPCOS-TDK, R 22.1/13.7/7.9). Fig. 3 presents the core temperature measured with a NTC thermistor (Littelfuse, PS104J2 [16]) and an IR camera (FLIR, A655sc [17], 30 frames/sec). In addition, the temperatures $T_{core,sim}$ and $T_{NTC,sim}$ are depicted, as extracted from a simulation of the circuit of Fig. 2. For the implementation of the simulation circuit the values of $C_{th,core}$, $R_{th,leak}$, and τ_{NTC} need to be known. In this regard, $C_{th,core}$ is determined in advance (cf. Sec. III-A) and $R_{th,leak}$ is estimated with (4) during the cooling phase of the measurement. The time constant of the NTC, $\tau_{NTC} = 5.5\,\mathrm{s}$, is determined such that the difference between simulated and measured waveforms is minimal.

It is found that simulated and measured waveforms match for both measurements, i.e., core and NTC temperatures. Moreover, the resulting simulated model was further used and successfully reproduced the temperature waveforms of the same experimental setup for different induced core losses, ranging from 0.4 W to 4.5 W, which further verifies the applicability of the considered circuit.

III. MEASUREMENT ACCURACY

An error analysis reveals different sources of inaccuracies for the proposed procedure:

- Limited accuracy of the measurement of the thermal capacitance, $C_{th,core}$.
- Temperature gradient in the core, due to non-homogeneous magnetic flux distribution (and finite thermal conductivity of the core material).
- Thermal time constant, $\tau_{th,NTC}$, and limited accuracy of the temperature measurement.
- Uncertainty of heat flux leaking to the ambient and to the winding by means of thermal conduc-

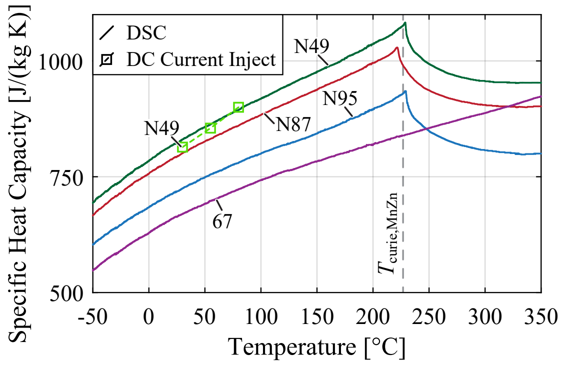

Fig. 4. Measured specific heat capacities of N87, N97 and N49 MnZn ferrite materials of EPCOS-TDK and 67 NiZn ferrite material of Fair-Rite using the Differential Scanning Calorimeter (DSC) 2500 of TA instruments. Additionally, for three different temperatures (30 °C, 55 °C, and 80 °C), the specific heat capacity of N49 is measured according to [21], where the ferrite conducts a DC current for generating a defined ohmic power loss in order to heat up. With known DC losses, temperature rise, and core weight, the specific heat capacitance can be calculated.

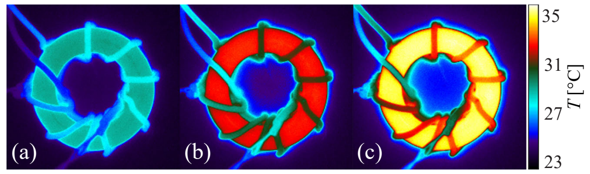

Fig. 5. Temperature monitoring of a toroidal ferrite core (R 22.1/13.7/7.9, N49) that is subject to a sinusoidal flux of 500 kHz and 100 mT, using the FLIR A655sc IR camera. The three depicted frames correspond to the temperatures (a) 29 °C, (b) 32 °C, (c) 35 °C. For all temperatures the maximum deviation between the points of lowest and highest temperatures in radial direction of the core is below 0.3 °C.

tion, convection, and radiation (modeled with $R_{\text{th,leak}}$).

- Temperature dependency of the core losses.
- Cross-coupling between the winding and the core losses.

In the following, these sources of inaccuracies are discussed.

A. Accuracy of core's thermal capacitance

Accurate knowledge of $C_{\text{th,core}}$ is of high importance, since it directly influences the calculated losses, cf. (1). Out of different measurement methods proposed in literature, the Differential Scanning Calorimetry (DSC) [18] features the best trade-off between complexity and accuracy. The basic operating principle of this method relies on the accurate measurement of the heat flow that is provided to a given sample in order to achieve a defined increase of the sample's temperature, which enables the calculation of its differential specific heat capacity as a function of temperature. The employed DSC 2500, from TA Instruments [19], uses a sapphire sample as reference and provides a measurement accuracy of ±2 %.

Fig. 4 depicts the specific heat capacities of three MnZn ferrite materials (N87, N97, and N49 of EPCOS-TDK) and of one NiZn ferrite material (67 of FairRite). The specific heat capacities of all four materials are temperature dependent, which is a known property of ferrite. The abrupt steps for MnZn materials at approximately 215 °C correspond to the Curie temperature [20].

DSCs are commonly used in material science, however, they may be less accessible in power electronics. An alternative, more accessible way, for the measurement of $C_{\text{th,core}}$ is discussed in [21]: a sample of the considered material is used as a DC electric conductor and, by means of Joule heating, the thermal response of the core is used to determine $C_{\text{th,core}}$ using (1). For the sake of completeness, this method has also been applied to the N49 material at three different ambient temperatures and the results are matching very well with the results obtained with the DSC (max. deviation of 3.0 %, cf. Fig. 4).

The temperature dependency of $C_{\text{th,core}}$ is an unwanted property for transient calorimetric loss measurements. However, the core temperature is only subject to minor changes of less than 10 °C during the measurements and accordingly the corresponding change of the thermal capacitance is minor (less than 1.5 %).

B. Impact of core's thermal resistance

Thermal imaging (cf. **Fig. 5**) confirms that the temperature gradient inside the core is negligible, due to the relatively high thermal conductivity of ferrite ($\lambda \geq 3.5\,\text{W/(mK)}$). Therefore, $R_{\text{th,core}}$ can be omitted (cf. Fig. 2(a)). As a result, and similar to the electric measurement, the investigated procedure does not measure the local (potentially inhomogeneous) loss density but rather the total losses of the considered core.

C. Inaccuracy due to NTC time constant

For the temperature measurement, the PS104J2 NTC thermistor of Littelfuse [16] is used. In order to achieve a fast NTC response and at the same time mechanical robustness, the temperature sensor is glued on the core using a thermally conductive adhesive (8329TFM-25ML of MG Chemicals). Generally, an uncoated core is preferred, and in case of coating, the coating is carefully locally removed, even though its impact on the measured response is minor.

The achieved time constant varies between 1-6 s. However, the impact of the time constant of the NTC sensor is minimized for $t_1 > 2\tau_{\text{NTC}}$ (and $t_2 > t(\max(T_{\text{NTC}})) + 2\tau_{\text{NTC}}$ during the cooling phase) and the introduced error is below 1 %. This together with the variation of τ_{NTC} between different cores is why τ_{NTC} is not included in the loss-extraction process (cf. (3), (6)).

D. Inaccuracy due to temperature measurement error

An interface circuit is employed to process the resistance change of the NTC thermistor and achieves an accuracy of ±0.05 °C for the measurement of temperature differences. Accordingly, and with respect to (5), the relative error of the measured core losses decreases for increasing temperature difference, $T_{\mathrm{meas}}(t_1 + \Delta t_1) - T_{\mathrm{meas}}(t_1)$, and reaches values of less than 2 % for temperatures differences greater than 5 °C.

E. Accuracy of $R_{th,leak}$

The impact of $R_{\mathrm{th,leak}}$ on the extracted losses is found to be small, since $t_{\mathrm{off}} \ll R_{\mathrm{th,leak}} C_{\mathrm{th,core}}$. In addition, its estimation is an integral part of the measurement procedure. A detailed analysis reveals that the maximum relative uncertainty of the measured core losses, which arise from a worst-case estimation error of $R_{\mathrm{th,leak}}$, is less than 1 %.

F. Temperature dependency of the core losses

The losses of ferrite materials are highly temperature dependent. The proposed method measures, per definition, the average value of the losses generated within the measurement interval. Therefore, the measurement time should be kept small such that the temperature increase is less than 10 °C.

G. Impact of winding losses

Winding losses potentially cause additional heating of the core, which needs to be limited. In this regard, the winding losses need to be at least one order of magnitude less than the core losses, which is found to be easily achieved with proper choice of the CUT design parameters (e.g., core geometry, number of turns, type of conductor). In order to further minimize this effect, a thermally isolating interface tape (≈ 0.3 mm) can be placed between the winding and the core. The impact of the distance of winding and core on the flux inside the core is negligible, especially for MnZn ferrite materials, whose relative permeability typically exceeds 1000. This is also verified experimentally using a single-turn sensing winding. Comparison between the voltage applied to the excitation winding and the measured sense winding voltage (scaled with the turns ratio) resulted in a perfect match.

H. Correlation between voltage and flux

The correlation between the applied voltage and the considered core flux density has a general impact on the determined core losses. Conversion of the induced flux into flux density is conventionally done by division of the flux by the cross section of the employed core. However, cores (toroids) typically employed for the measurement of core losses result into flux density differences between the inner and outer radius of 60-70 %. This difference raised to a typical power of $\beta \approx 2.5$ results in a ratio of the maximum and the minimum losses in radial core direction of more than 3. Therefore, it is advised to consider cores with slim profile in order to ensure limited flux density differences and accordingly an approximately homogeneous loss distribution in the CUT.

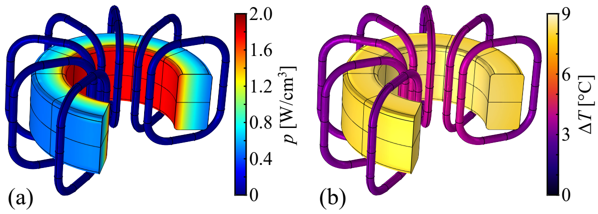

Fig. 6. FEM simulation results of a toroidal ferrite core (R 22.1/13.7/7.9, N49) with 10 turns (high frequency litz wire, 180 × 71 µm), for the specifications of the experiment of Fig. 3, i.e., 500 kHz/100 mT and average core losses equal to 1.53 W. The depicted result corresponds to the instant $t = t_{\mathrm{off}}$. (a) Loss density distribution, (b) temperature distribution.

I. Experimental guideline

In the course of a basic guideline, t_1 and Δt_1 are the two user-defined variables that define the accuracy of the experiment. In order to minimize the impact of the NTC's time constant, t_1 is set equal to $2\tau_{\mathrm{NTC}}$; in order to mitigate the error of the temperature measurement sensor, Δt_1 that results in a $\Delta T_{\mathrm{core}} \approx \Delta T_{\mathrm{NTC}}$ greater than 100 times the differential measurement accuracy of the equipment (for the presented case $\Delta T_{\mathrm{meas}} \geq 100 \times 0.05\,°\mathrm{C} = 5\,°\mathrm{C}$) is chosen. Larger values of ΔT_{meas} introduce additional error mostly due to the temperature dependency on the core losses, but also due to the (minor) temperature dependency of $C_{\mathrm{th,core}}$ and $R_{\mathrm{th,leak}}$.

IV. FEM Simulation

In order to verify the validity of the method in more detail, a 3D FEM simulation (COMSOL Multiphysics software [22]) of the core losses and the temperature distribution of the experimental setup has been conducted (cf. **Fig. 6**). The model is solved in a two-step process, starting from a frequency domain magnetic field problem, followed by a heat transfer problem in the time-domain. Critical dependencies, i.e., core-loss density with respect to flux and temperature, specific heat capacity with respect to temperature, and the dependencies of different cooling mechanisms (convection and radiation) on temperature are taken into consideration. The modeled specifications correspond to the experiment depicted in Fig. 3 featuring a toroidal core (R 22.1/13.7/7.9) made of N49 MnZn ferrite material with 10 turns of high-frequency litz wire (180 × 71 µm) which is subject to a sinusoidal flux with a frequency of 500 kHz and an average flux density of 100 mT.

The resulting temperature progression over time is in good agreement with the core temperature behavior of the simulated circuit, $T_{\mathrm{core,sim}}$, of Fig. 3.

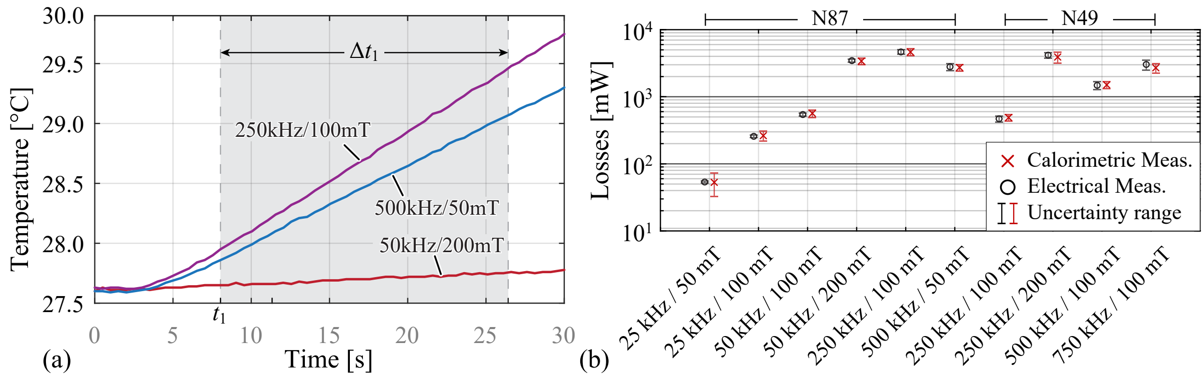

Fig. 7. (a) Comparison of the temperature progression over time of three different measurements of Ferrite N87; (b) Comparison of the measured losses of the proposed calorimetric and the electric method described in [5] for two different CUTs, i.e., R 41.8/26.2/12.5 - N87 and R 22.1/13.7/7.9 - N49.

Furthermore, as discussed in Sec. III-H, the FEM simulation reveals a substantial gradient of the core loss density in radial direction (cf. Fig. 6(a)) with a ratio of maximum to minimum loss density of 3.8. However, the impact on the core temperature gradient is negligible ($T_{core,max} - T_{core,min} < 0.3$ °C, cf. Fig. 6(b)), which further confirms the assumption of $R_{th,core} \approx 0$. Additionally, the fact that the winding losses are at least an order of magnitude lower compared to the core losses is also verified. The deviation between the core losses estimated with (4), (5) and the average core losses over time ($t \in (t_1, \Delta t_1)$) of the FEM simulation is 5 %.

V. Experimental verification

Figure 7 depicts measured temperatures and core losses for ferrite N87 and N49 (EPCOS-TDK) that have been obtained with a setup according to Fig. 1. The two CUTs were an R 41.8/26.2/12.5 (N87) and an R 22.1/13.7/7.9 (N49), with 15 and 10 turns of excitation winding, respectively. For the excitation winding a high-frequency litz wire 180 × 71 µm was employed. Moreover, the temperature was measured as proposed in Sec. III-C. In order to verify the accuracy of the measurement, electrical measurements are conducted as an alternative to the proposed method, employing capacitive compensation of the inductive behavior as described in [5] and shown in Fig. 8. For this concept, in addition to the capacitive compensation, a sense winding directly connected to a high input impedance voltage probe is used, that is not influenced by R_{coil1}, i.e., the winding losses. Finally, a high accuracy measurement of the circuit current, i_{meas}, allows for calculation of the core losses of the CUT using

$$P_{CUT} = i_{meas,rms} v_{meas,rms}. \tag{6}$$

For each measured point an error analysis was conducted for both methods in order to verify the accuracy of the measurements. The average absolute deviation between the two methods for all measurements is less than 5.0 % and the maximum

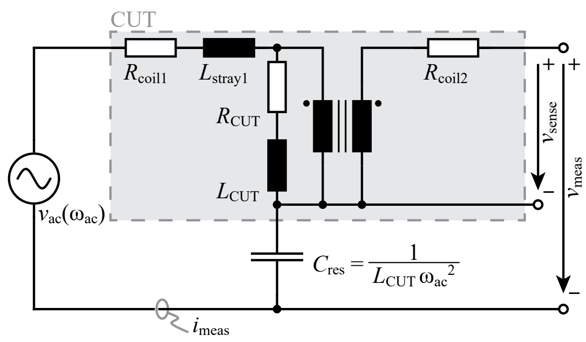

Fig. 8. Electrical circuit, according to [5], used together with the proposed transient calorimetric method, for the accuracy verification of the measurement of core losses presented in Fig. 7(b).

absolute deviation is below 13.0 %, both of which confirm the validity of the method. More interestingly the method is successfully applied to a substantially wide range of losses between 45 mW-4.5 W. Finally, it can be observed that with increasing frequency the uncertainty range of the electrical measurements, even for the case of capacitive compensation of the reactive power, starts exceeding the one of the proposed method, mainly due to the error introduced by the measurement equipment. This confirms the significance of the transient calorimetric method especially for measurements in the MHz range.

VI. Conclusion

This paper presents a transient calorimetric method for measuring the losses of ferrite cores independent of the type of excitation, with or without premagnetization. The method relies upon the correlation between the measured rate of rise of the core temperature over time, the core's thermal capacitance and the introduced losses. The main sources of inaccuracy are discussed and supported based on a proposed equivalent circuit, FEM simulations and thermal imaging using a high resolution IR camera.

The method is applied on commonly used N87 and N49 MnZn ferrite materials of EPCOS-TDK, and measurement results are verified by electrical measurements. For all measurements, the deviation between the measured and the reference values is below 13 %, which is within the typical tolerance of cores produced in different batches, but also within the commonly accepted accuracy for the execution of a complete component optimization.

ACKNOWLEDGMENT

The authors would like to thank Dr. Kirill Feldman of the Soft Materials Laboratory of ETH Zurich, for supporting this work with providing his expertise in materials science and for conducting the specific heat capacity measurements using the Differential Scanning Calorimeter method. Furthermore, the comprehensive support of the Fair-Rite Products Corporation (Mr. John Lynch) with samples of NiZn ferrite cores, detailed core loss data and further core material characteristics is thankfully acknowledged. Finally, the authors are very grateful to the Rudolf-Chaudoire-Foundation for supporting the participation of PhD students in leading Power Electronics conferences.

REFERENCES

[1] B. Carsten, "Waveforms for stimulating magnetic cores," *Presentation at the PSMA Magnetics Committee / IEEE PELS High Frequency Magnetics Workshop*, March 2017.

[2] V. J. Thottuvelil, T. G. Wilson, and H. A. Owen, "High-frequency measurement techniques for magnetic cores," in *Proc. of the IEEE Power Electronics Specialists Conf. (PESC)*, June 1985, pp. 412–425.

[3] B. Carsten, "Fast, accurate measurement of core loss at high frequencies," in *Proc. of the Int. Conf. on Power Conversion and Intelligent Motion (PCIM)*, March 1986, pp. 29–33.

[4] J. Zhang, G. Skutt, and F. C. Lee, "Some practical issues related to core loss measurement using impedance analyzer approach," in *Proc. of the IEEE Applied Power Electronics Conf. and Expo. (APEC)*, vol. 2, March 1995, pp. 547–553.

[5] Z. Daming, S. Birlasekaran, S. T. Tang, and H. P. Cheng, "Ferrite core loss measurement with arbitrary wave excitation," in *Proc. of the IEEE International Conf. on Power System Technology (PowerCon)*, vol. 1, Nov. 2004, pp. 564–567.

[6] M. Mu, F. C. Lee, Q. Li, D. Gilham, and K. D. T. Ngo, "A high frequency core loss measurement method for arbitrary excitations," in *Proc. of the IEEE Applied Power Electronics Conf. and Expo. (APEC)*, March 2011, pp. 157–162.

[7] M. Mu, Q. Li, D. J. Gilham, F. C. Lee, and K. D. T. Ngo, "New core loss measurement method for high-frequency magnetic materials," *IEEE Trans. Power Electron.*, vol. 29, no. 8, pp. 4374–4381, Aug 2014.

[8] C. R. Sullivan, "Survey of core loss test methods," (accessed July 19, 2019). [Online]. Available: http://sites.dartmouth.edu/power-magnetics/files/2017/03/Survey-of-Core-Loss-Test-Methods-Sullivan.pdf

[9] D. Hou, M. Mu, F. C. Lee, and Q. Li, "New high-frequency core loss measurement method with partial cancellation concept," *IEEE Trans. Power Electron.*, vol. 32, no. 4, pp. 2987–2994, April 2017.

[10] F. Zhu, Q. Li, and F. C. Lee, "Improved partial cancellation method for high frequency core loss measurement," in *Proc. of the IEEE Applied Power Electronics Conf. and Expo. (APEC)*, March 2019, pp. 1430–1435.

[11] T. Kleeb, B. Dombert, S. Araújo, and P. Zacharias, "Loss measurement of magnetic components under real application conditions," in *Proc. of the IEEE European Power Electronics and Application Conf. (EPE-ECCE Europe)*, Sep. 2013, pp. 1–10.

[12] P. Papamanolis, F. Krismer, and J. W. Kolar, "Minimum loss operation of high-frequency inductors," in *Proc. of the IEEE Applied Power Electronics Conf. and Expo. (APEC)*, March 2018, pp. 1756–1763.

[13] C. Xiao, G. Chen, and W. G. H. Odendaal, "Overview of power loss measurement techniques in power electronics systems," *IEEE Trans. Ind. Appl.*, vol. 43, no. 3, pp. 657–664, May 2007.

[14] J. K. Bowman, R. F. Cascio, M. P. Sayani, and T. G. Wilson, "A calorimetric method for measurement of total loss in a power transformer," in *Proc. of the IEEE Power Electronics Specialists Conf. (PESC)*, June 1991, pp. 633–640.

[15] T. Komma and H. Gueldner, "A method of determining core losses caused by a DC flux-density bias," in *Proc. of the Int. Conf. on Power Conversion and Intelligent Motion (PCIM)*, March 2002, pp. 215–220.

[16] "PS104J2 - PS Series," (accessed Nov. 19, 2019). [Online]. Available: https://www.littelfuse.com/products/temperature-sensors/leaded-thermistors/interchangeable-thermistors/standard-precision-ps/ps104j2.aspx

[17] "HIGH-RESOLUTION SCIENCE GRADE LWIR CAMERA - FLIR A655sc," (accessed Oct. 08, 2019). [Online]. Available: https://www.flir.com/products/a655sc/

[18] G. W. H. Hohne, W. F. Hemminger, and H.-J. Flammersheim, "Differential scanning calorimetry," *Springer*, 2003.

[19] "DSC 2500 - Discovery DSC Series," (accessed Nov. 12, 2019). [Online]. Available: https://www.tainstruments.com/dsc-2500/

[20] "EPCOS Data Book 2013 - Ferrites and Accessories," (accessed Nov. 19, 2019). [Online]. Available: https://www.tdk-electronics.tdk.com/download/519704/069c210d0363d7b4682d9ff22c2ba503/ferrites-and-accessories-db-130501.pdf

[21] D. Neumayr, D. Bortis, J. W. Kolar, S. Hoffmann, and E. Hoene, "Origin and quantification of increased core loss in MnZn ferrite plates of a multi-gap inductor," *CPSS Transactions on Power Electronics and Applications*, vol. 4, no. 1, pp. 72–93, March 2019.

[22] "COMSOL Multiphysics® v. 5.4." (COMSOL AB, Stockholm, Sweden). [Online]. Available: www.comsol.com